Supporting Information

Charge Transport Dynamics of $C_6H_4NH_2CuBr_2I/TiO_2$ Heterojunction in Aqueous Solution Under Reverse Bias

Pujia Cheng,[1] Wenjing Lv,[1] Kaidong Zhan,[1] Zhili Shi,[1] Yaqi Liu,[1] Fan Wu,*[1] Quinn Qiao*[2]

[1]Huzhou Key Laboratory of Materials for Energy Conversion and Storage, School of Science, Huzhou University, Huzhou, 313000, China

[2]Mechanical and Aerospace Engineering, Syracuse University, Syracuse, NY 13244, United States

Corresponding Authors * (F.W.) E-mail: wufan@zjhu.edu.cn

(Q.Q.) E-mail: quqiao@syr.edu

Experimental

Film fabrication

The FTO substrates were cleaned through ultrasonication using soap, deionized water, acetone, and isopropanol for 30 min each, followed by treatment with UV-ozone for 30 min. Subsequently, 0.010 g of copper acetate hydrate dissolved in 5 mL of anhydrous ethanol to prepare the CuO precursor. Then, TiO_2 compact layer was obtained by spin-coating (4500 rpm, 60 s) diisopropoxy titanium diacetylacetonate in ethanol (0.15 M) on FTO conductive glass, and then annealed at 150 °C for 5 min and 450 °C for 30 min on hot plate. TiO_2 mesoporous layer was fabricated by spin-coating (5000 rpm, 45 s) TiO_2 paste (dispersed TiO_2 slurry in absolute ethanol with volumn ratio 1:6) on TiO_2 compact layer, and annealed at 120 °C for 10 min, 200 °C for 5 min, 300 °C for 5 min, and 460 °C for 15 min. $C_6H_4NH_2I$ (0.274 g) and $CuBr_2$ (0.279 g) were dissolved in N, N-dimethylaminamide (0.5 mL) by agitating at 70°C, and the solution was rested overnight. The combined solution was subjected to ultrasonication for 30 min before being filtered through PTFE syringe filters (0.22 μm). An TiO_2-covered FTO substrate was spin-coated with a $C_6H_4NH_2CuBr_2I$ solution at 4000 rpm for 60 s in a glovebox. This was followed by annealing for 30 min on a hot plate at 70°C.

Characterization

A field emission scanning electron microscope (FE-SEM) was used to characterize the morphology (ZEISS, GeminiSEM 300) of the material. An MXP18AHF X-ray diffractometer with Cu Kα irradiation (λ =1.54056 Å) was used to determine the phase. An ultraviolet spectrophotometer (UV-2600, Shimadzu, Japan) was used to analyze photon absorption. Photoelectrochemical performance was analyzed using a three-electrode cell with the supporting electrolyte of 0.5 M of Na_2SO_4 aqueous solution. Our film covered FTO substrate was working electrode, Pt sheet was used as counter electrode and Ag/AgCl was used as the reference electrode. Photocurrent–time response curves (*i-t*) with repeated light on and off were carried out on the electrochemical workstation (IviumStat.h, Netherlands) under the chopped light of a white LED (P_s=11.5 mW/cm^2). IMPS measures the periodic photocurrent response of the cell to a small sinusoidal perturbation of the light intensity superimposed on a broader steady background level. IMPS is a powerful technique for the analysis of the charge carrier dynamics, providing essential clues on how to improve photo-electrochemical systems for their application. This techniques lead to the determination of a time constant for the frequency-dependent photocurrent response, which is a

signature of a specific transport or recombination process occurring in the device.[1,2] The intensity-modulated photocurrent spectroscopy (IMPS) were obtained using the same electrochemical workstation (IviumStat.h, Netherlands) and white light-emitting diodes with an unsteady light intensity P_{in} (= $P_s\delta e^{i2\pi ft}$) as background illumination. The small sinusoidal perturbation depth δ is 10% on P_s with the frequency range from f= 15000 to 0.01Hz.

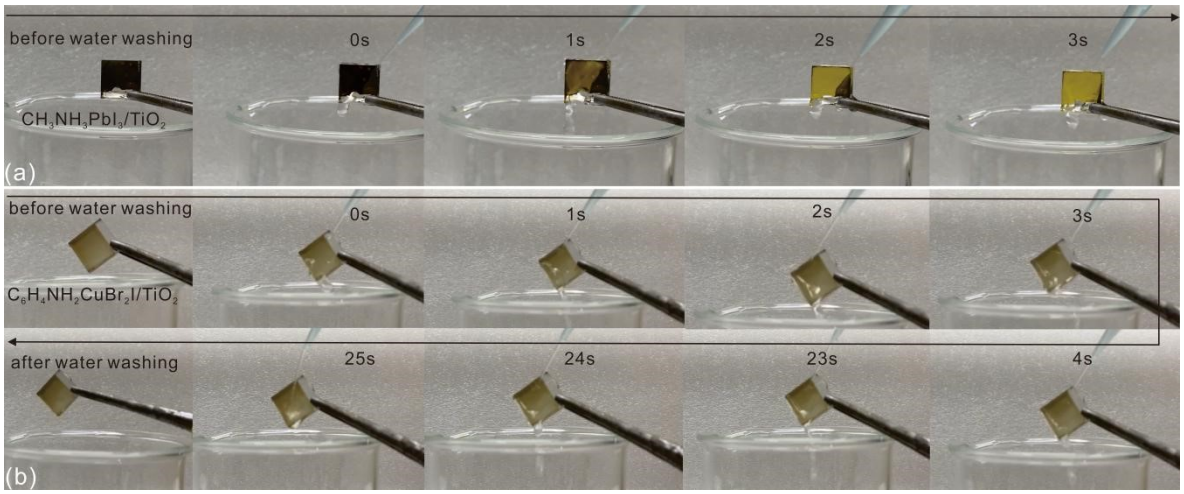

Figure S1. The digital photos of changes of (a) $CH_3NH_3PbI_3/TiO_2$ and $C_6H_4NH_2CuBr_2I/TiO_2$ samples after repeated water washing with 3s and 25s, respectively.

As shown in Figure S1a, the star perovskite $CH_3NH_3PbI_3/TiO_2$ sample was immediately decomposed after contacting water; while our prepared $C_6H_4NH_2CuBr_2I/TiO_2$ film did not show any decomposition after repeated water washing for 25s as shown in Figure S2b, and the corresponding UV-vis absorption did not change significantly in Figure 1c in the text.

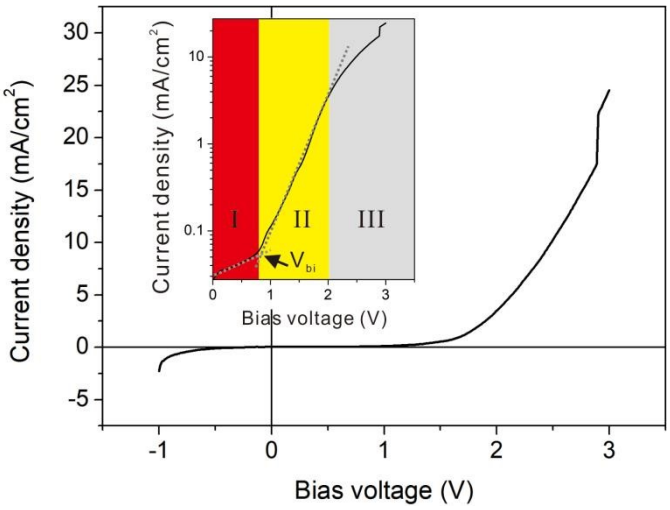

Figure S2. The linear plots of *J-V* characteristic of $C_6H_4NH_2CuBr_2I/TiO_2$ heterojunction, in which, the inset is the semilogarithmic *J-V* plot.

We measured the dark *J-V* of $C_6H_4NH_2CuBr_2I/TiO_2$ sample in photoelectrochemical cell. The linear *J-V* plot is shown in Figure R2, which performed the typical heterojunction rectifying performance.[3] Moreover, the corresponding semilogarithmic plot was also analyzed (as shown in the inset of Figure R2). Normally, the dark *J-V* characteristic of heteojunction exhibits three distinct regimes:[4,5] (I) linear increase for leakage dominated current, (II) exponential increase for diffffusiondominated current, and (III) quadratic increase for spacecharge-limited current. The built-in voltage (V_{bi}) of heterojunction could be evaluated at the point where the dark *J-V* curve begins to follow a quadratic behavior. Obviously, the measured semilogarithmic *J-V* plot is very consistent with above three regions, which further confirms that heterojunction is formed in $C_6H_4NH_2CuBr_2I/TiO_2$ sample.

The conduction band energy (E_c) and valence band energy (E_v) of the $C_6H_4NH_2CuBr_2I$ are −4.76 and −6.40 eV, respectively, while the E_c and E_v of TiO_2 are −4.20 eV and −7.40 eV, respectively. Tt forms a type-II (staggered) band alignment between $C_6H_4NH_2CuBr_2I$ and TiO_2 according to the energy level matching, which has been proved to be effective in promoting the interfacial charge-transfer process.[6] Becasue a built-in electric field could be formed across the heterojunction interface (as shown in the Figure S2). The built-in electric field is helpful for a more efficient electron-hole pairs separation at the electrochemical interface.[7,8]

In additional, the current indeed droped at the initial cycles until 5000 s in Figure 2a, and this phenomenon was more significant with a higher reverse bias. This phenomenon is very common in

photoelectrochemical cells.[9-12] When a semiconductor is illuminated with light having an energy larger than the semiconductor bandgap, the energy of the photons can be absorbed and excited electrons and holes are generated in the conduction and valence band, respectively. When these photoexcited electrons or holes are in the space charge region they migrate toward the electrode surface where they participate in charge transfer reactions giving a photocurrent. Photocurrents caused by photogenerated electrons (cathodic currents) or holes (anodic current) are negligible when they are the majority charge carriers. Under these conditions, their concentration is barely increased by photoexcitation. However, their photocurrent becomes significant when the reacting electrons or holes are minority charge carriers. In this case their concentration is greatly increased by photoexcitation as compared with the concentration of the minority charge carriers in the absence of radiation (in the dark). Therefore, photocurrents can only be observed with reactions in which the participating carriers are minority charge carriers. This means transfer of holes at n-type electrodes and electrons at p-type electrodes leading to anodic and cathodic photocurrents, respectively. As reported by Lin et al., the photocurrent in photoelectrochemical cells was composed of three steps: **(i) the photocurrent appeared promptly**, which is associated with the generation of charges under light irradiation, **(ii) the photocurrent decreased sharply**, which is associated with the the recombination of photogenerated electron-hole pairs and **(iii) the photocurrent reached a steady state**, which is associated with the balance of generation and recombination of photogenerated electron–hole pairs.[12]

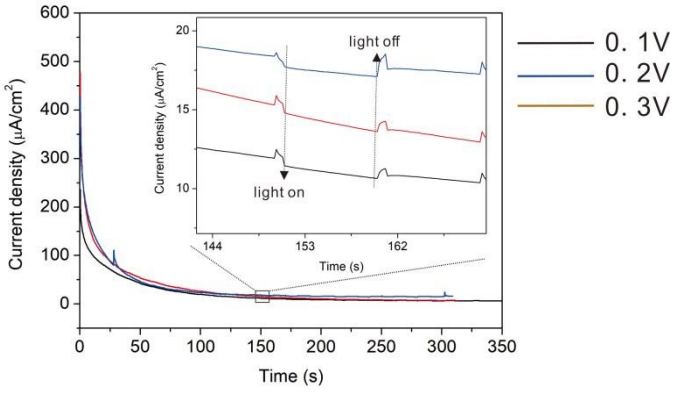

Figure S3. The *i-t* curves of $C_6H_4NH_2CuBr_2I/TiO_2$with different forward bias under chopped white light.

As shown in Figure R1, the photocurrent was weak when bias shifting toward positive values. This can be explained by a decrease in the space charge region allowing a less efficient electron-hole

pairs separation at the electrochemical interface.[13] Meanwhile, the IMPS signal under forward bias became very bad when the photocurrent was very weak, which caused a distorted and even anomalous Nquist plot. Therefore, it is hard to study the effect of forward bias on charge dynamics.

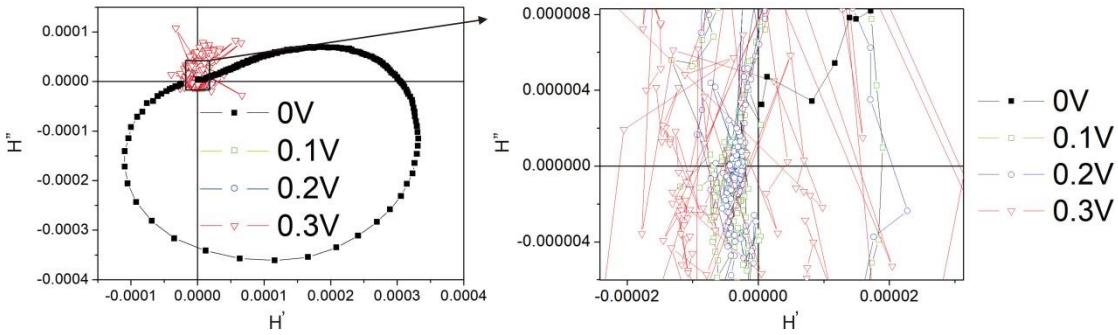

Figure S4. The IMPS plot of $C_6H_4NH_2CuBr_2I/TiO_2$ based photoelectrochemical cells under 0−0.3V bias.

When a bias is applied on photoelectrode, the external electric field across the heterojunction may provide additional driving force for charge transport. When the bias< 0 V, the external electric field will make the electrons and holes drift away from the heterojunction interface due to the same direction as their diffusions. Therefore, a reverse electric field (E_r) favors the movement of both electrons and holes toward the respective electrodes; while a forward bias will result in a forward electric field (E_f) that drives the carriers to drift toward the heterojunction interface in the direction reverse to their diffusions. Obviously, the E_r will facilitate the interfacial electron-hole pairs dissociation and the charge transport to electrodes, while the E_f will impose an opposite effect on these processes. In order for IMPS to reflect the information of photogenerated charges, the total current (J_L=J_{ph}+J_D) under light must be almost equal to the photogenerated current (J_{ph}), that is, the contribution of dark current (J_D) should be very less which could be ignored.[14]

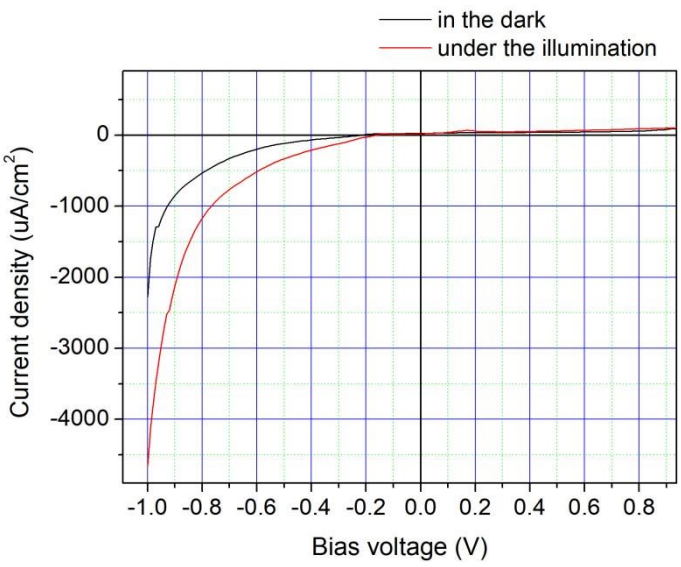

Figure S5. The *J*−*V* curves of $C_6H_4NH_2CuBr_2I/TiO_2$ based photoelectrochemical cells that measured in the dark and under illumintation (white light-emitting diodes with an intensity of 11.5 mW/cm^2), respectively.

Known from our *J*-*V* measurements in **Figiure S4**, the dark current J_d is much lower than the total current J_L when bias voltage ≤ -0.3V. It is reasonable to consider that the contribution of the J_d to the measured current J_L can be ignored during the IMPS measurements with applied a voltage in the range of -0.3V, i.e., $J_L \approx J_{ph}$. Therefore, the changes in the IMPS responses within the bias voltage range do reflect the applied voltage effects on the transport dynamics of photogenerated charges. However, when the bias voltage ≥ -0.4V, the dark current J_d gradually apporaches to the same orders of magnitude of the total current J_L. Therefore, the IMPS plots cannot reflect the information of photogenerated charges when J_d has big contribution to the J_L.[14,15] Moreover, the dark current starts to increase exponentially when reverse bias >0.3 V, which means that the heterojunction is gradually broken down. Therefore, we did not increase the reverse bias to a higher voltage than -0.3 V when studying IMPS. In addition, we also tried to measure the IMPS under higher voltages than -0.3 V as shown **Figure R4**. Obviously, when the bias is higher than -0.3 V, the semicircle in the low frequency range in the 1st quadrant that correlated with the microscopic dynamic process is disappeared. Instead, the *RC* attenuation in the 2nd and 3rd in the high frequency range that correlated with macroscopic dynamical process becomes prominent.[16] Therefore, we did not increase the reverse bias to a higher voltage than -0.3 V when studying IMPS.

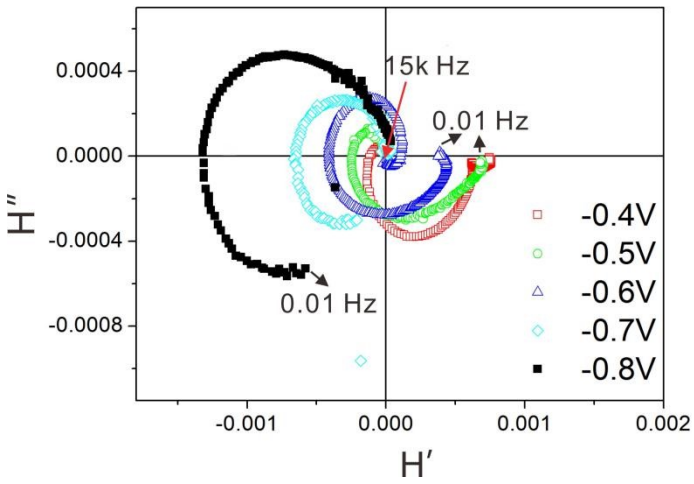

Figure S6. IMPS plots of $C_6H_4NH_2CuBr_2I/TiO_2$ heterojunction based photoelectrochemical cells that measured under bias voltages from -0.4 V to -0.8 V.

Table S1. The calculated diffusion dynamic parameters of $C_6H_4NH_2CuBr_2I/TiO_2$ photoelectrode from IMPS under no bias.

	k_t (s^{-1})	k_{rec} (s^{-1})	τ_t (ms)	τ_{rec} (ms)	L (nm)
$C_6H_4NH_2CuBr_2I/TiO_2$	0.57	22.85	1741.91	43.76	23.77

The effective charge diffusion coefficient D and the charge transport time constant τ_t (the reciprocal of k_t) were related as follows:[17]

$$\tau_t = d^2/4D \quad (2)$$

Furthermore, the charge diffusion length L was then calculated as follows:[18]

$$L=(D\times\tau_r)^{1/2} \quad (3)$$

τ_r is the charge recombination time constant(the reciprocal of k_{rec}). Using equations (2) and (3), L was evaluated as ~23.77 nm in the $C_6H_4NH_2CuBr_2I/TiO_2$ photoelectrode.

References:

[1] Y. Wang, W. Tian, C. Chen, W. Xu and L. Li, *Advanced Functional Materials*, 2019, **29**, 1809036.

[2] P. Vecchi, A. Piccioni, R. Mazzaro, M. Mazzanti, V. Cristino, S. Caramori and L. Pasquini, *Solar RRL*, 2022, **6**, 2200108.

[3] E. C. Anderson,T. L. Bougher and B. A. Cola, *Advanced Electronic Materials*, 2018, **4**, 1700446.

[4] P. Ruankham, L. Macaraig, T. Sagawa, H. Nakazumi and S. Yoshikawa, *The Journal of Physical Chemistry C,* 2011,115, 23809.

[5] V. D. Mihailetchi, P. W. M. Blom, J. C. Hummelen and M. T. Rispens, *Journal of Applied Physics*, 2003, **94**, 6849.

[6] X. D. Wang, Y. H. Huang, J. F. Liao, Y. Jiang, L. Zhou, X. Y. Zhang, H. Y. Chen and D. B. Kuang, *Journal of the American Chemical Society*, 2019, 141, 13434.

[7] K. Rahimi, *Physical Chemistry Chemical Physics*, 2020, 22, 7412.

[8] S. Wang, C. Ren, H. Tian, J. Yu and M. Sun, *Physical Chemistry Chemical Physics*, 2018, 20, 13394.

[9] J. P. Kollender, J. Gasiorowski, N. S. Sariciftci, A. I. Mardare and A. W. Hassel, *The Journal of Physical Chemistry C*, 2014, **118**, 16919.

[10] A. Paracchino, V. Laporte, K Sivula, M. Grätzel and E.Thimsen, *Nature materials*, 2011, **10**, 456.

[11] Z. Li, W. Zhang, Q. Zhao, H. Gu, Y. Li, G. Zhang, F. Zhang and X. Fan, *ACS Sustainable Chemistry & Engineering*, 2015, **3**, 468.

[12] M. Wang, L. Sun, Z. Lin, J. Cai, K. Xie and C. Lin, *Energy Environ. Sci.*, 2013, 6, 1211.

[13] J. P. Kollender, J. Gasiorowski, N. S. Sariciftci, A. I. Mardare, and A. W. Hassel, *The Journal of Physical Chemistry C*, 2014, **118**, 16919.

[14] C. Chen, R. Peng, H. Wu and M. Wang, The Journal of Physical Chemistry C, 2009, 113, 12608.

[15] P. M. DiCarmine, O. A. Semenikhin, *Electrochimica Acta*, 2008, **53**, 3744.

[16] I. Rodriguez-Gutierrez, E. Djatoubai, J. Su, A. Vega-Poot, G. Rodriguez-Gattorno, F. L. Souza and G. Oskam, *Solar Energy Materials and Solar Cells*, 2020, **208**, 110378.

[17] J. Halme, K. Miettunen, P. Lund, *The Journal of Physical Chemistry C* 2008, **112**, 20491.

[18] J. Krüger, R. Plass, M. Gratzel, P. J. Cameron, L. M.Peter, *The Journal of Physical Chemistry B* 2003, **107**, 7536.